REPORT DOCUMENTATION PAGE

Form Approved OMB NO. 0704-0188

1. REPORT DATE (DD-MM-YYYY)	2. REPORT TYPE	3. DATES COVERED (From - To)
04-09-2016	Final Report	1-Sep-2010 - 31-Aug-2014

4. TITLE AND SUBTITLE
Final Report: Investigation of Voltage-Activated BAW Devices and Filters

5a. CONTRACT NUMBER
W911NF-10-1-0286

5b. GRANT NUMBER

5c. PROGRAM ELEMENT NUMBER
611102

5d. PROJECT NUMBER

5e. TASK NUMBER

5f. WORK UNIT NUMBER

6. AUTHORS
Robert York

7. PERFORMING ORGANIZATION NAMES AND ADDRESSES
University of California - Santa Barbara
3227 Cheadle Hall
3rd floor, MC 2050
Santa Barbara, CA 93106 -2050

8. PERFORMING ORGANIZATION REPORT NUMBER

9. SPONSORING/MONITORING AGENCY NAME(S) AND ADDRESS (ES)
U.S. Army Research Office
P.O. Box 12211
Research Triangle Park, NC 27709-2211

10. SPONSOR/MONITOR'S ACRONYM(S)
ARO

11. SPONSOR/MONITOR'S REPORT NUMBER(S)
58188-EL.10

12. DISTRIBUTION AVAILIBILITY STATEMENT
Approved for Public Release; Distribution Unlimited

13. SUPPLEMENTARY NOTES
The views, opinions and/or findings contained in this report are those of the author(s) and should not contrued as an official Department of the Army position, policy or decision, unless so designated by other documentation.

14. ABSTRACT
The overarching goal of this project was to better understand and exploit voltage-induced piezoelectricity in thin-film strontium titanate (STO) and barium-strontium titanate (BST), with the ultimate objective of creating high-performance, reconfigurable filters and frequency-agile RF components. Unlike conventional BAW technology, the piezoelectric coupling in BST is controlled by an applied DC field. In the absence of a DC field no acoustic resonance is observed; when a DC field is applied the device becomes piezoelectrically active and acts like a high-

15. SUBJECT TERMS
bulk acoustic wave, BAW, resonator, tunable dielectrics, RF switch

16. SECURITY CLASSIFICATION OF:			17. LIMITATION OF ABSTRACT	15. NUMBER OF PAGES	19a. NAME OF RESPONSIBLE PERSON
a. REPORT	b. ABSTRACT	c. THIS PAGE			Robert York
UU	UU	UU	UU		19b. TELEPHONE NUMBER 805-895-2562

Standard Form 298 (Rev 8/98)
Prescribed by ANSI Std. Z39.18

RPPR
as of 06-Oct-2017

Agency Code:

Proposal Number:

Agreement Number:

Organization:
Address: , ,
Country:
DUNS Number:
EIN:
Report Date:
Date Received:
for Period Beginning and Ending
Title:
Begin Performance Period:
End Performance Period:
Report Term: -
Submitted By:
Email:
Phone:

Distribution Statement: -

STEM Degrees:
STEM Participants:

Major Goals:

Accomplishments:

Training Opportunities:

Results Dissemination:

Plans Next Period:

Honors and Awards:

Protocol Activity Status:

Technology Transfer:

Investigation of Voltage-Activated BAW Devices and Filters

Final Report

Award Information:
Contract Number: W911NF1010286
Period of Work: Sep 1, 2010 to Aug 31, 2014
UNIVERSITY OF CALIFORNIA, SANTA BARBARA
Santa Barbara, 931062050, USA
Principal Investigator: Dr. York, Robert , rayork@ece.ucsb.edu, phone: 805-895-2562

1 Objectives

The overarching goal of this project was to better understand and exploit voltage-induced piezoelectricity in thin-film strontium titanate (STO) and barium-strontium titanate (BST), with the ultimate objective of creating high-performance, reconfigurable filters and frequency-agile RF components. Unlike conventional BAW technology, the piezoelectric coupling in BST is controlled by an applied DC field. In the absence of a DC field no acoustic resonance is observed; when a DC field is applied the device becomes piezoelectrically active and acts like a high-Q BAW resonator, a fundamental building block for frequency-selective circuits. This effective was first discovered and examined under an earlier ARO-funded program (W911NF0610431), and the present project was intended to further the understanding and identify refinements in processing, and device design/layout,that would result in significant improvements in the prior state-of-the-art. In particular, loss contributions from device parastics and interface quality were examined and improved, and initial filter circuits were realized with improved devices. Characterization of the device behavior over temperature and different RF power levels was also explored in this program. Further improvement in the technology will require a focus on improving the BST material quality and interface roughness. Among other possibilities this new technology allows for a new class of filters that would address a critical need in modern communication systems.

Key Terms/Abbreviations/Acronyms:
BAW: Bulk Acoustic Wave
VBAW: Voltage-Activate Bulk Acoustic Wave (technology proposed herein)
ABR: Acoustic Bragg Reflector. A high reflectivity “mirror” for acoustic waves formed using alternating layers of high and low impedance materials.
SMR: Solidly-Mounted Resonator: a BAW device fabricated on an ABR.
FBAR: Film Bulk Acoustic Device: A BAW device suspended on a thin membrane.
BST: Barium Strontium Titanate
STO: Strontium Titanate

2 Accomplishments

2.1 Improved Device Design with Patterned Mirrors

The acoustic Bragg reflectors (ABR) used in our work consist of four quarter-wavelength alternating high and low acoustic impedance layers. For simplicity and convenience, a pair of Pt/SiO_2 layers has been used in our SMR devices, although in a practical device more layers would be preferred to yield a higher reflection coefficient. Earlier work had identified sources of loss that were limiting performance associated withparasitic resistances and capacitances in the underlying mirror structure. A new device design was proposed to address these issues using a patterned mirror structure. This was explored using two identical devices fabricated on different mirrors.

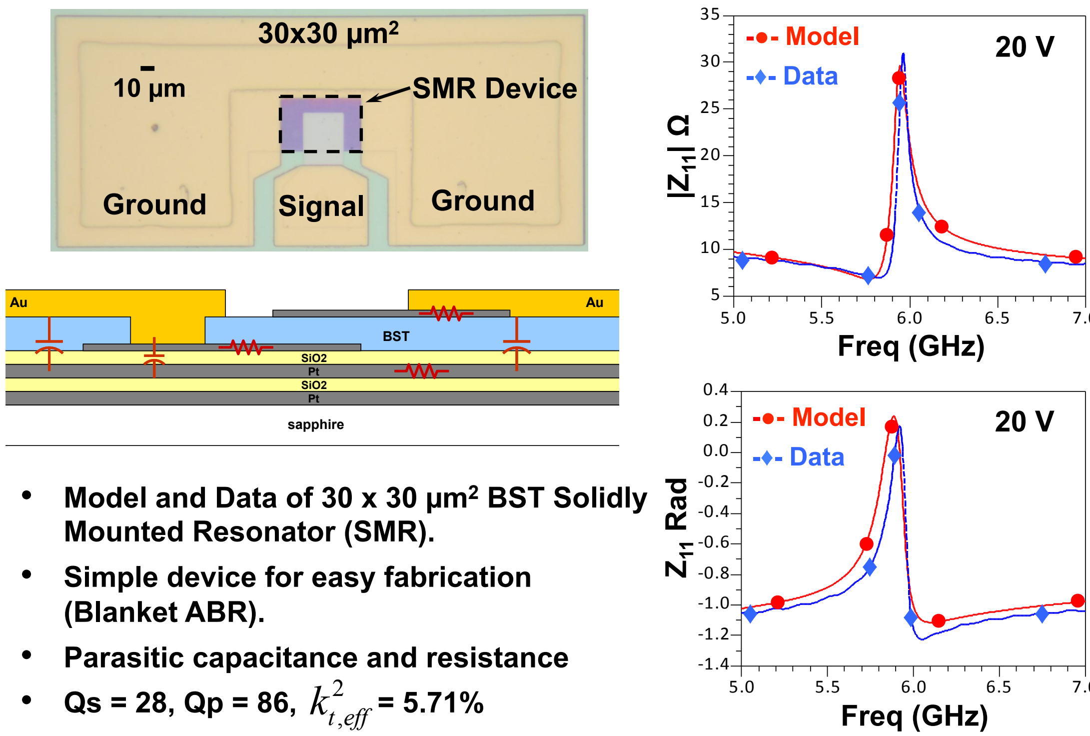

Figure 1: Device structure on unpatterned ABR, identifying key parasticis. The measured magnitude and phase of the impedance is shown around the resonance point at 20 V applied DC bias. The BVD model prediction is shown for comparison.

Figure 1 illustrates the original device structure using a blanket ABR, along with measured data. The one-port scattering parameters were measured using a Cascade Microtech probe station, GGB GSG probes, and an E8361A vector network analyzer. The collected data was fitted to the Butterworth-Van Dyke (BVD) model and the quality factor of the resonators was calculated using $Q_{r,a} = (f/2)\,d\varphi/df$, where φ is the phase of the input impedance, and the derivative with respect to frequency is evaluated at the resonant and antiresonant frequencies. The effective electromechanical coupling coefficient was calculated by $k^2_{t,eff} = \pi^2 (f_a - f_r)/4f_a$. The figure identifies sources of resistance and parasitic capacitance in the structure that limit the performance

Figure 2 shows the improved device structure using a patterned ABR, implemented by liftoff prior to BST deposition. The quality factors of the voltage acitivated BST SMRs with patterned and unpatterned ABRs are $Q_r = 55$ and $Q_a = 116$, and $Q_r = 28$ and $Q_a = 86$ respectively, at 20 V applied bias. The data clearly shows a significant improvement in the quality factor between the device with patterned and unpatterned ABR. Also the effective electromechanical coupling coefficient was calculated by $k^2_{t,eff} = \pi^2 \left(f_a - f_r\right) / 4 f_a$ to be 6.51% and 5.71% for the patterned and unpatterend ABR devices respectively, at 20V applied bias. This result is significant in demonstrating that the losses are not all associated with the BST material itself, but also influenced significantly by the quality of the ABR and other device parastics. Further improvements in device Q would therefore be expected by using more aggressive lithography to shrink access resistances in the electrodes, and additional layers in the ABR to improve the reflection coefficient.

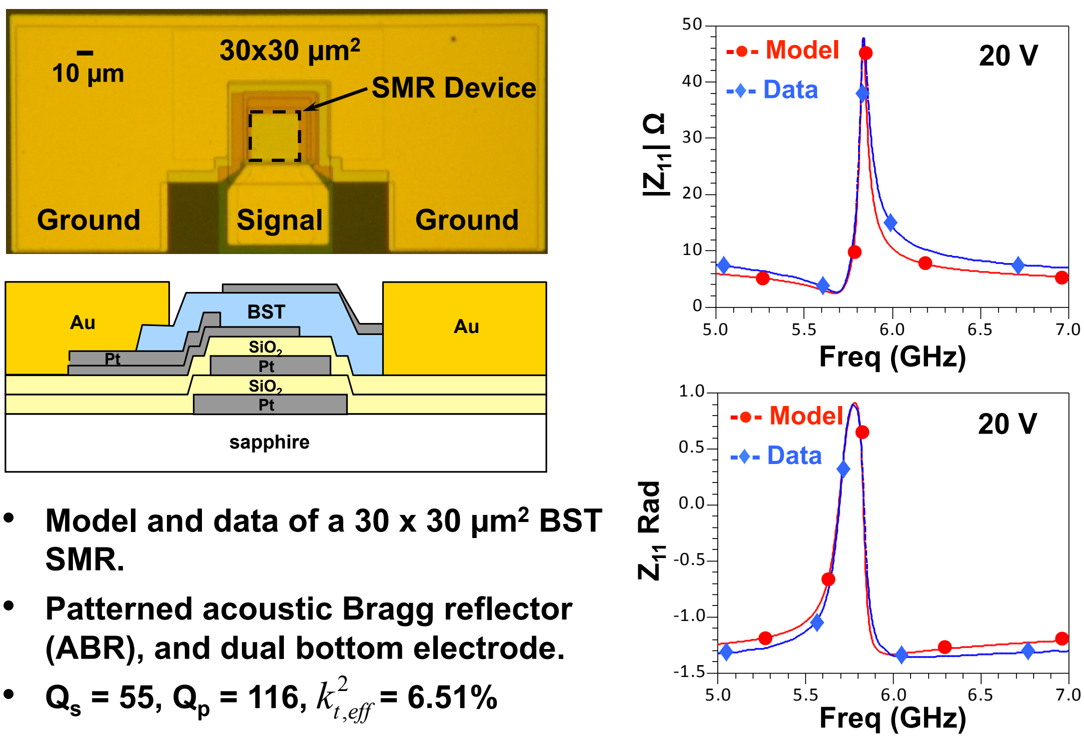

Figure 2: New device structure on a patterned ABR formed by liftoff prior to BSt deposition. The measured magnitude and phase of the impedance is shown around the resonance point at 20 V applied DC bias. The BVD model prediction is shown for comparison. The new device structure yields significant improvements in device quality factors.

2.2 Initial Circuit Demonstrations

Our first attempt at fabricating voltage activated BST bulk acoustic wave filters yielded encouraging results. A ladder structure filter composed of a series and shunt bulk acoustic wave resonators, and a capacitively coupled solidly mounted resonator filter were fabricated. The L-section building block of a ladder filter is illustrated schematically in Figure 3 (top), and the narrow band RF data for the ladder structure filter are summarized in the figure and showing good agreement between the model vs. data. At 0V bias the filter behaves as a series and shunt capacitors, however when a dc bias voltage is applied, 10 V in this case, we observe a band pass filter response at the approximately 6GHz. The insertion loss and return loss were measured to be -4.26 dB and -13.5 dB, respectively. The 3dB bandwidth of the filter was measured to be 72 MHz and the quality factor of the filter was calculated by $Q = f_0 / BW_{3dB}$ to be 84, where f_0 is the center frequency and BW_{3dB} is the 3dB bandwidth. Also shown are the wideband characteristics of the filter from 3-9GHz, showing approximately 5.25 dB of isolation between the on and off states and 4 dB of out-of-band rejection with respect to the center frequency.

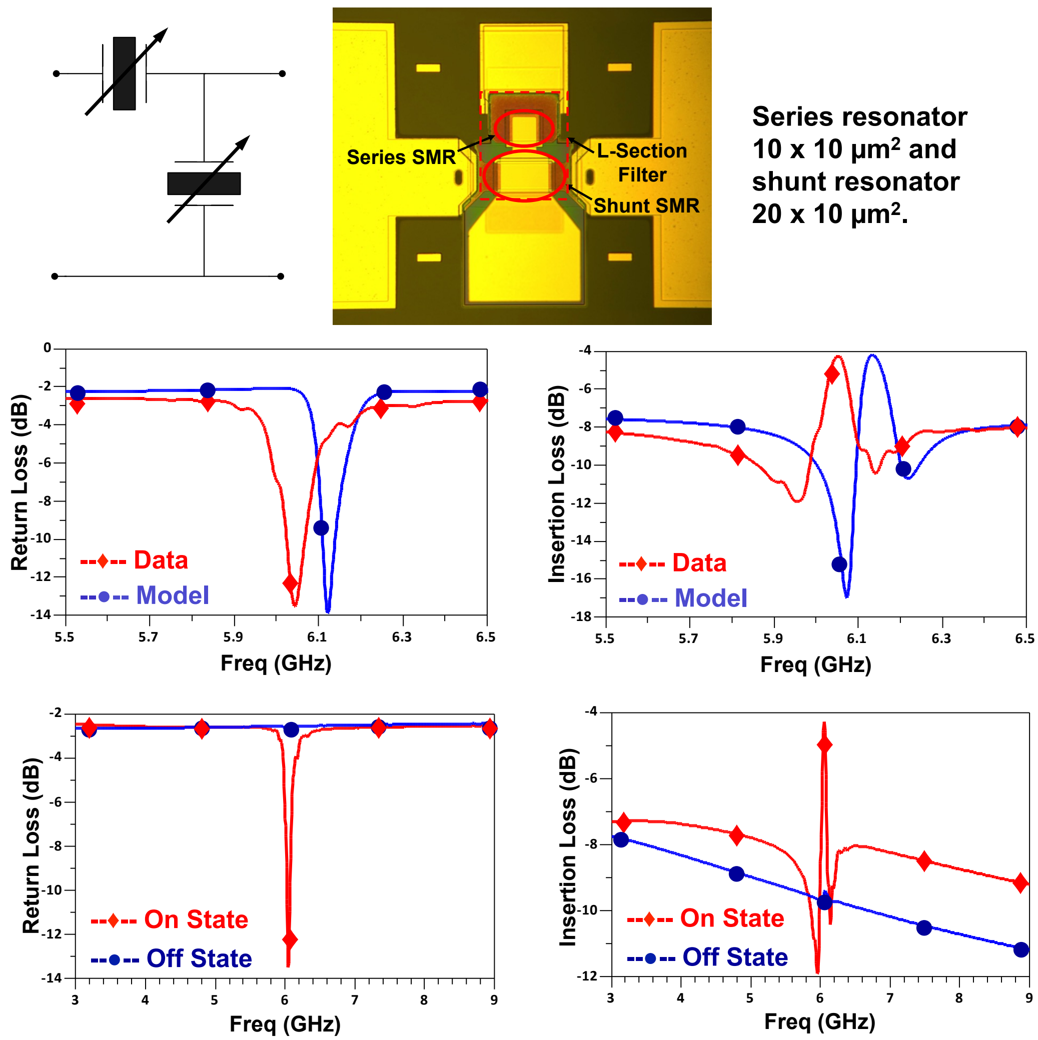

Figure 3: Schematic diagram and photograph of fabricated (a) one section ladder structure VBAW BST SMR filter and (b) capacitively coupled BST SMR filter. Wide band two port scattering parameters on and off characteristic for voltage activated BST SMR filter at 10V dc bias.

Practical filters would be constructed of a large cascade of these L-section blocks. For example, a typical FBAR device used in cellular communications has nine or more sections cascaded, resulting in much higher isolation and sharper frequency selectivity. Figure 4 illustrates how the response changes when additional devices are cascaded to form a ladder structure, using the modeled data from Figure 3. The out-of-band rejection and on-off isolation improve as more sections are cascaded, however the insertion loss also increases, highlighting a key area for future improvement in this technology.

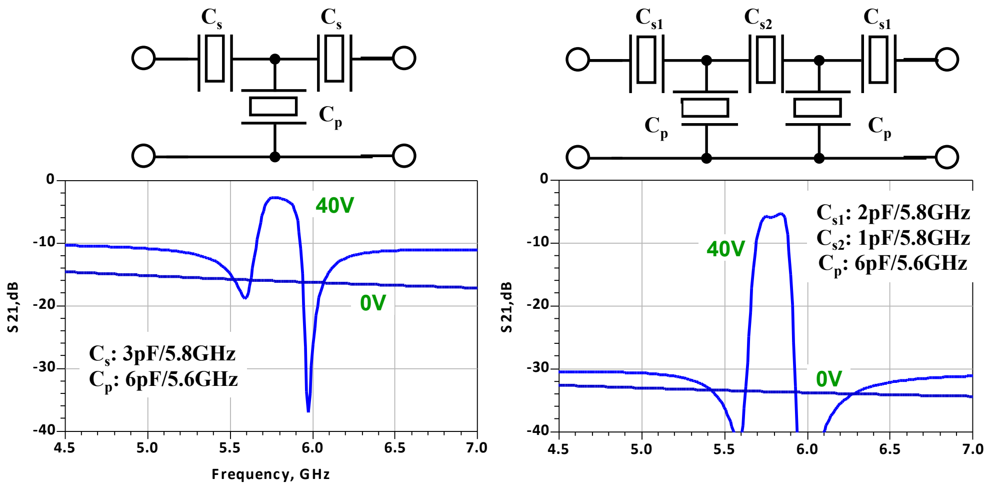

Figure 4: Predicted response of larger ladder structures, using the model fitted to experimental data in Figure 3.

Figure 5 shows the capacitively coupled solidly mounted resonator structure, along with the two port scattering parameters for a capacitively coupled 15x15 μm^2 BST SMR filter biased at 30 V. The measured insertion loss of the filter is -3.66 dB and the return loss is -13.74 dB. At the resonant frequency there is 35 dB of rejection with respect to the antiresonant frequency. Also illustrated is the on and off states of the filter and approximately 20 dB of isolation between the on state and the off state. This voltage activated BST BAW filter technology demonstrates a new direction for reconfigurable filters.

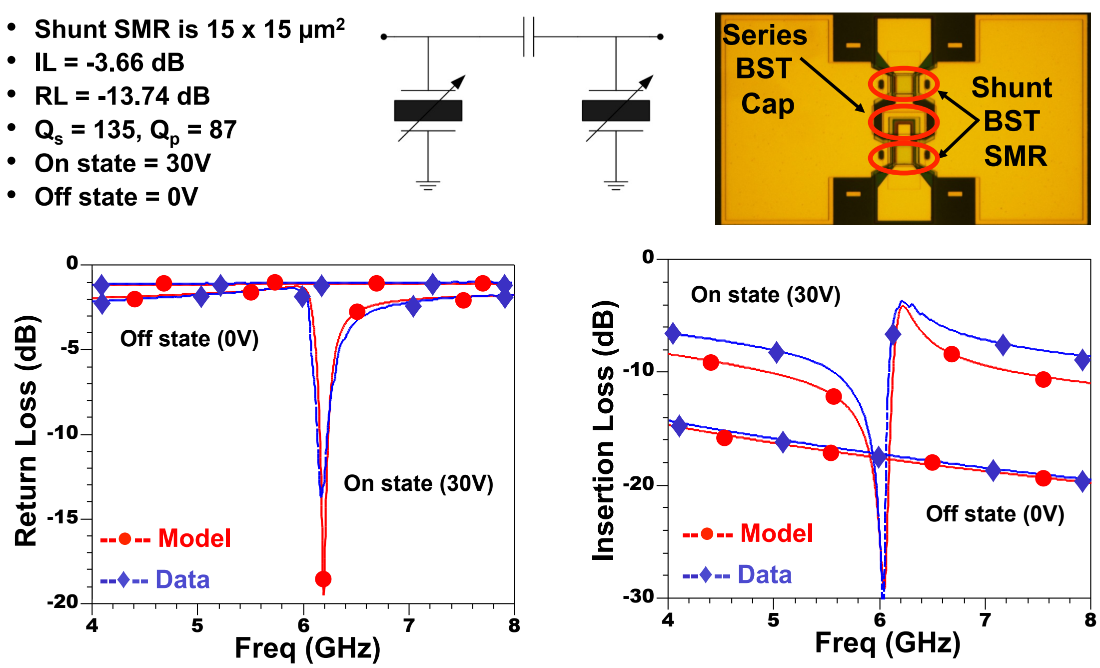

Figure 5: Capacitively coupled BST SMR filter two port scattering parameters data vs. model and on and off behavior.

2.3 Temperature-Dependence of Devices

Temperature dependent one-port scattering parameters were measured using a cryogenic RMC probe station, Cascade Microtech probe station, Cascade Mircotrech ACP 150μm GSG probes, and an E8361A vector network analyzer. The system was under vacuum (5.8e-5 Torr) prior to the start of measurements and the temperature was varied from 228K to 243K in 5K steps, from 245K to 293K in 2K steps, and from 298K to 393K in 5K steps. The data was collected on a 30x30 um2 device on patterned mirrors (Figure 6) over an applied dc bias of 0V to 30V in 5V increments.

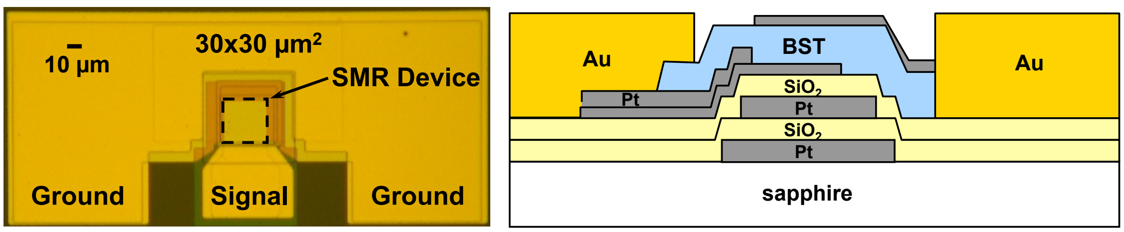

Figure 6: (a) Photograph of 30 x 30 μm^2 BST SMR with patterned ABR and (b) schematic of BST SMR with patterned ABR.

Figure 7 illustrates the variation of the series (left) and parallel (right) resonances frequency over temperature. The variation of the series and parallel resonant frequency normalized to the resonant frequency at 20°C is 0.83% and 0.73% at 30V, 0.73% and 0.69% at 25V, 0.97% and 0.6% at 15V, and 0.67% and 0.33% at 5V. The quality factor of the resonator was calculated using $Q_{r,a} = (f/2)\, d\varphi/df$, where φ is the phase of the input impedance, and the derivative with respect to frequency is evaluated at the resonant and antiresonant frequencies. Also the effective electromechanical coupling coefficient was calculated by $k_{t,eff}^2 = \pi^2 (f_a - f_r)/4 f_a$.

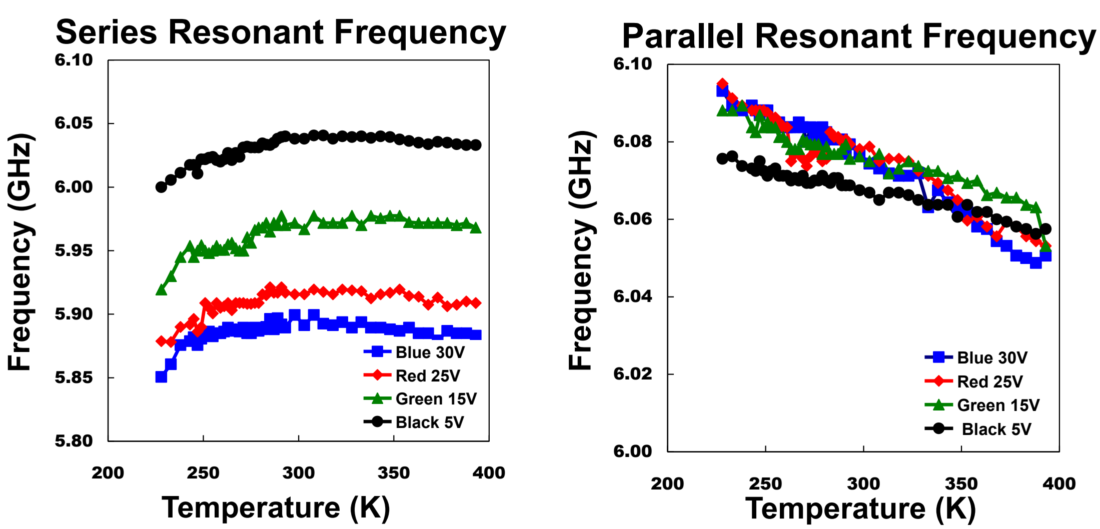

Figure 7: Series (left) and parallel (right) resonances frequency vs. temperature for four difference dc bias voltages 5V, 15V, 25V, and 30V.

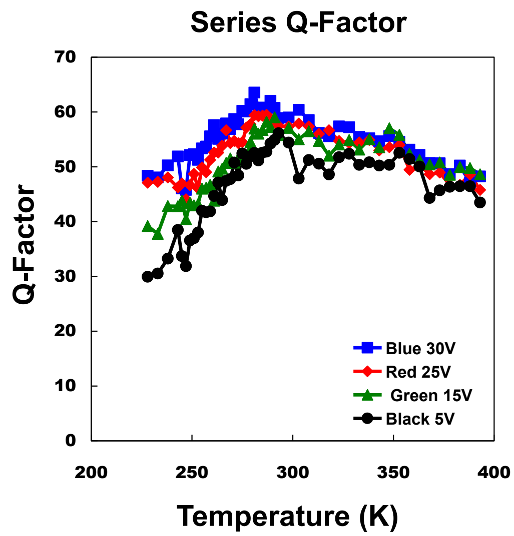

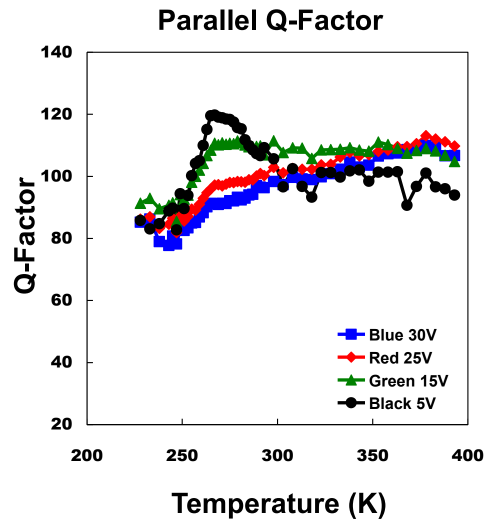

Figure 8: Series (left) and parallel (right) frequency effective quality factors vs. temperature for four different dc bias voltages 5V, 15V, 25, and 30V

Figure 8 shows the variation of the series and parallel resonance quality factors over out temperature range. The variation over temperature of the series and parallel resonance quality factor normalized to the quality factor at 20^{o}C is 30.2% and 54.7% at 30V, 26.8% and 54.2% at 25V, 38.1% and 46.5% at 15V, and 46.6% and 66.0% at 5V. Figure 9 illustrates the effective electromechanical coupling coefficient variation over temperature. This variation is normalized to the effective electromechanical coupling coefficient at 20^{o}C is 40.7% at 30V, 46.1% at 25V, 78.7% at 15V and 188.7% at 5V.

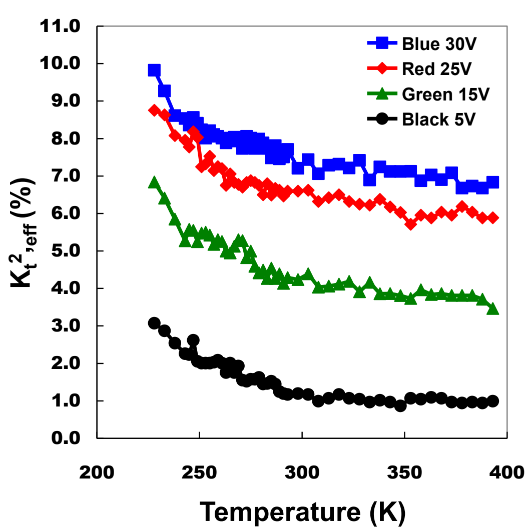

Figure 9: Effective electromechanical coupling coefficient vs. temperature for four different dc bias voltages 5V, 15V, 25V, 30V.

To appreciate the impact of these results on circuit performance, Figure 10 illustrates the temperature variation in the center frequency and insertion loss of the L-section filter of Figure 3 over select temperature points. The insertion loss increased with increasing temperature -4.27 dB at 233K to -4.98 dB at 393K. The frequency decreased with increasing temperature from 6.053 GHz at 233K to 6.046 GHz at 393K.

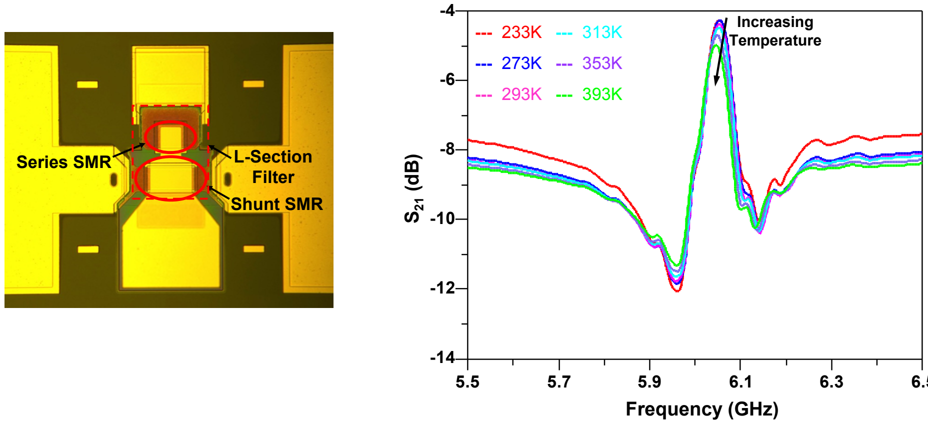

Figure 10: Picture of fabricated voltage activated BST SMR L-section filter (left) and temperature dependent scattering parameters for the BST voltage activated SMR filter in the on-state at 10V dc bias, at 233K, 273K, 293K, 313K, 353K, and 393K (right).

2.4 Nonlinearity and IMD Characterization

Large signal performance of the devices was investigated. The large signal performance is an important design consideration, since the likely end-use of these devices is in front-end filtering where the voltage swings can be quite high. Non-linear two port measurements were done using a Cascade Microtech probe station, Cascade Microtech ACP 150µm GSG probes, and an HP 8564 spectrum Analyzer. The measurement setup for the 1dB compression point and third order intercept point is illustrated in Figure 11. The measured 1dB compression points are 23dBm, 27dBm, and 24dBm and the output third order intercept points are 49dBm, 47.5dBm, and 42.5dBm at bias points, 0V, 15V, and 30V respectively. The measurements are illustrated in Figure 12. The data demonstrates good non-linear performance and a decrease in the 1dB compression point and third order intercept point with increasing bias. The abrupt change observed for the 30V bias case in Figure 12 at an input power of 22.5dBm per tone (roughly 6V peak-to peak signal swing) is due to the device failing at that combination of bias and power.

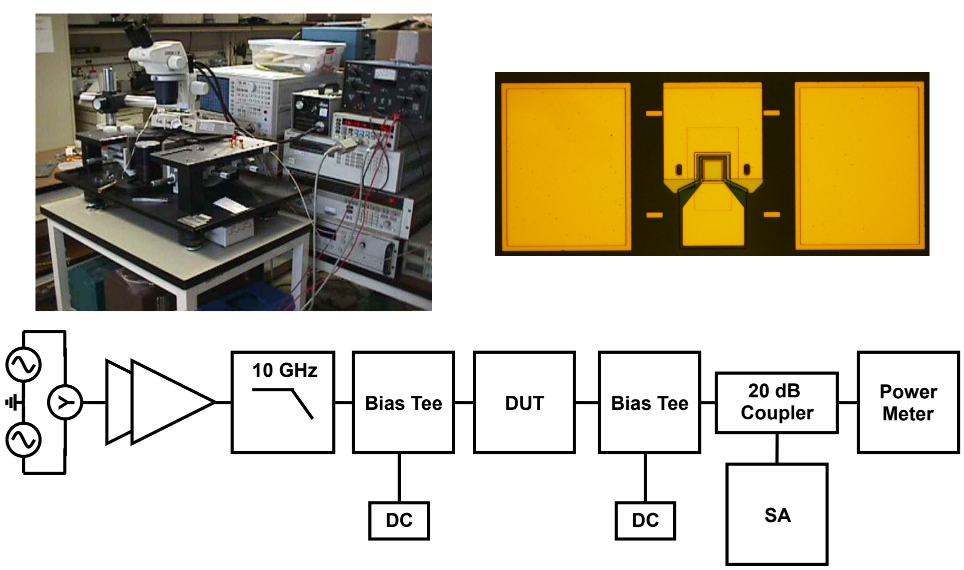

Figure 11: Photograph and block diagrams of the two-tone IMD measurement setup.

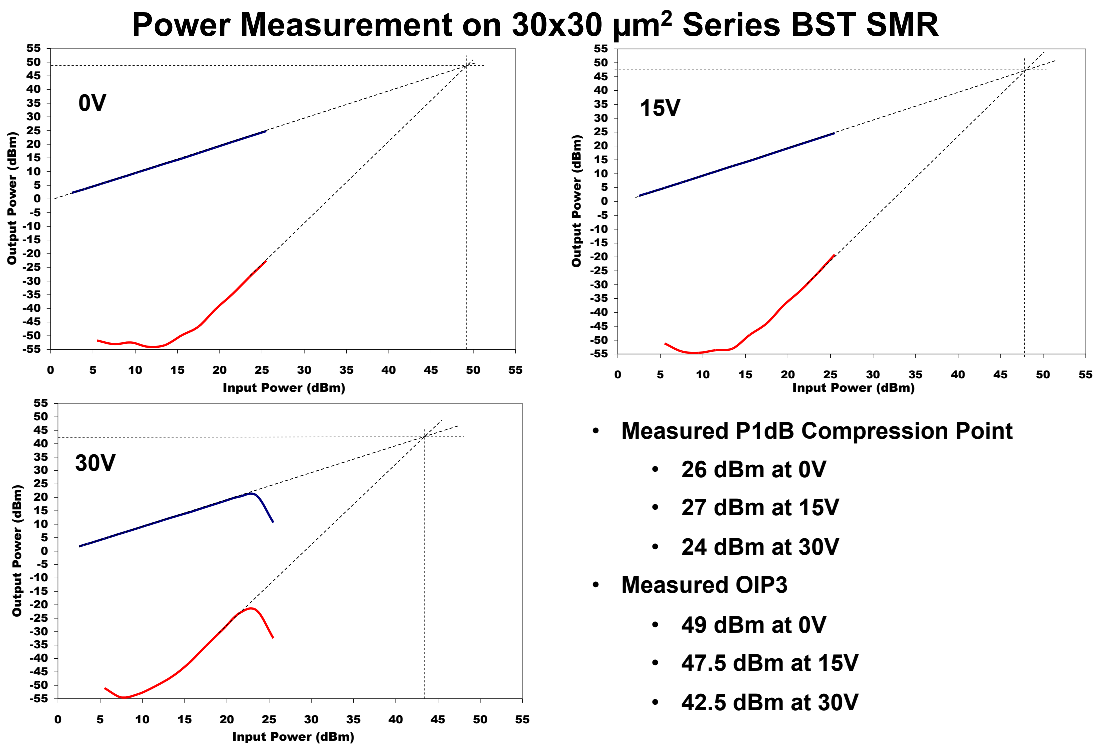

Figure 12: Plots of 1dB compression (top blue curve) and third order intercept point (bottom red curve) for voltage activated BST bulk acoustic wave solidly mounted resonator (a) 0V, (b) 15V and (c) 30V DC bias.

2.5 Importance of Surface Roughness on Q-factor

Aside from the parasitic losses discussed earlier, we have identified two other prominent loss mechanisms: surface roughness at the interfaces of the acoustic layers, which leads to scattering losses that scale directly with RMS roughness, and intrinsic losses in the material that relate to the material quality and crystal structure. To address the former issue we investigated a chemical mechanical polishing (CMP) process for our BST SMR devices. For simplicity a four layer blanket acoustic Bragg reflector was fabricated using alternating layers of Pt and SiO_2. Prior to starting the CMP the surface roughness of the top SiO_2 layer was measure by AFM (Figure 13, left) and after the CMP process the sample was measured again by AFM (Figure 13, right). The significant improvement in surface roughness are tabulated in the figure. To demonstrate the effectiveness of this processing step a simple SMR device was fabricated on top of both the unpolished and polished ABR surfaces. Figure 14 shows the scattering parameters and quality factor for a device fabricated on an unpolished ABR, and Figure 15 shows the one port scattering parameters for and q-factor for the device on the polished ABR. We see immediately a significant improvement in the quality factor due to the reduction in the surface roughness of the acoustic Bragg reflector. Further analysis showed that there is significant variation (26%) in the top surface SiO_2 thickness over the sample after Chemical Mechanical Polishing. To improve the resonator quality factor further we will reduce the top SiO_2 thickness variation to less then 10% by modifying the CMP process parameters, improve the interfacial roughness of the top BST layer by post deposition surface preparation by CMP at UCSB Nanofabrication facility, reduce acoustic damping losses in the ABR by exploring alternative materials and redesigning the ABR to account for shear-wave excitation.

	Before CMP		After CMP	
Location	RMS (nm)	Z-Range (nm)	RMS (nm)	Z-Range (nm)
1	4.602	35.354	0.504	3.745
2	4.670	38.137	0.611	5.002

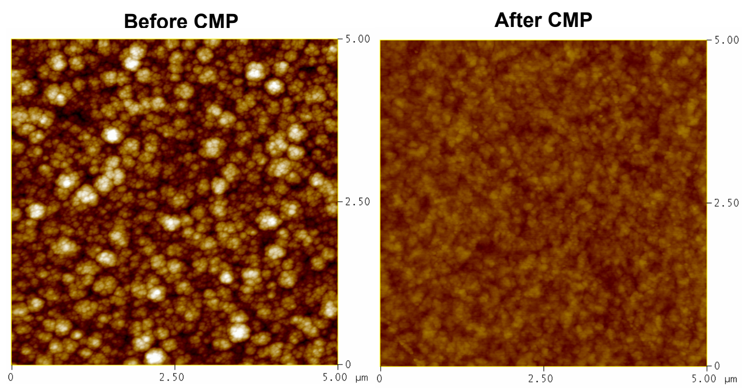

Figure 13: AFM images of unpolished (left) and polished (right) ABR SiO_2 layer. The measurements are tabulated in the top of the figure.

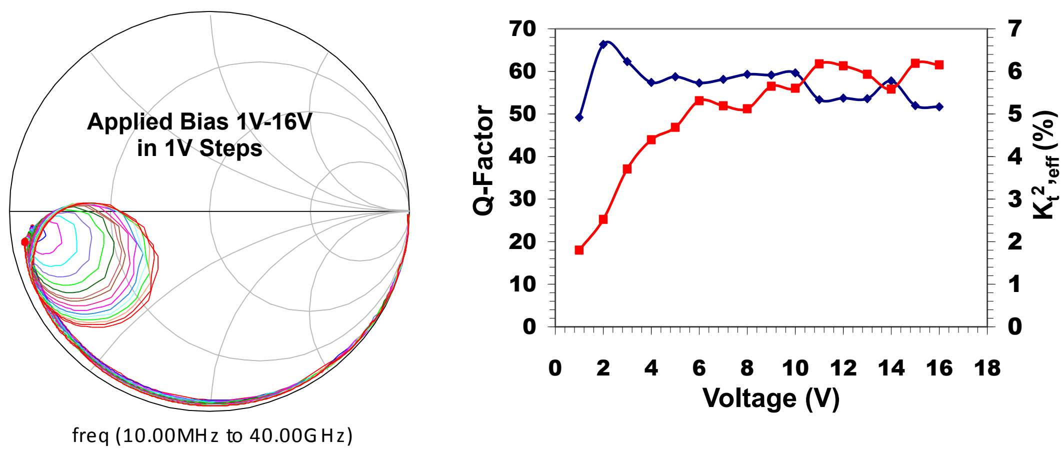

Figure 14: Scattering parameters (left) and quality factor (right) of a unpolished voltage activated BST SMR device.

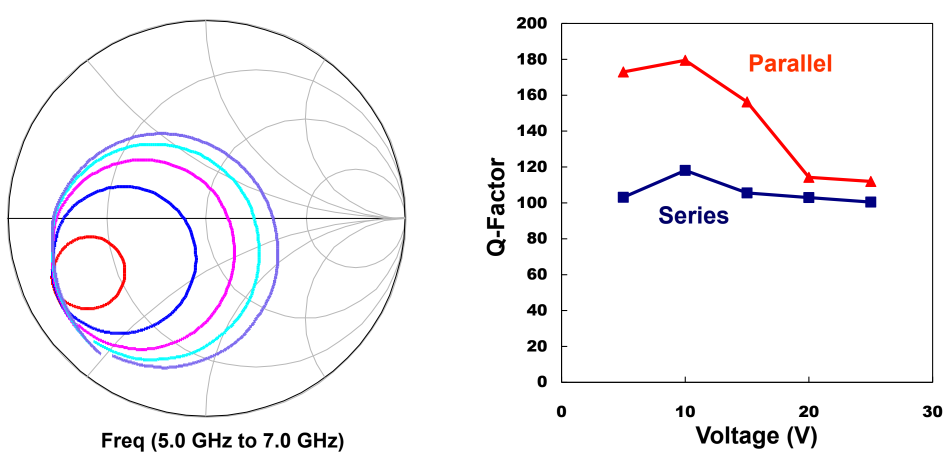

Figure 15: Scattering parameters (left) and quality factor (right) of a polished voltage activated BST SMR device.

To address intrinsic film losses, we have initiated an investigation of MBE-grown BST as the active layer for our devices, in collaboration with Prof. Stemmer at UCSB, . This new oxide-MBE capability yields BST thin films with quality factors in excess of 1000, corresponding to loss tangents of less than 0.001. A simple device was fabricated using MBE BST and the one port scattering parameters where measured. Figure 16 illustrates the device structure (top), the fitting of the data to the BVD model (left), and the effective electromechanical coupling coefficient which is 6.6% at 7V which is considerably higher when compared with sputtered BST. We believe that MBE materials could result in significant improvemenst in perfornace due to a combination of improved film quality (and hence lower instrinsic dielectric and acoustic losses), and improved surface roughness (atomically smooth surfaces). This could tbe the topic of a future investigation.

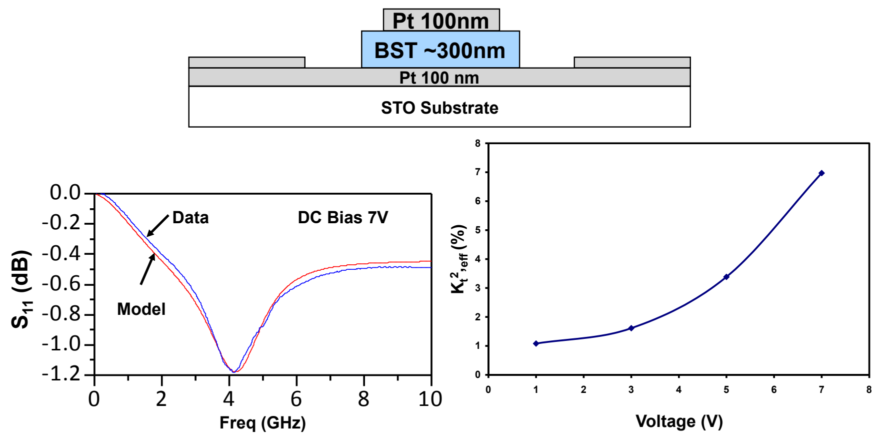

Figure 16: Device structure (top), BVD model vs. data (left), and effective electromechanical coupling factor (right).

3 Publications Arising from this work

1. The effect of patterned vs. unpatterned acoustic Bragg reflector on barium strontium titanate solidly mounted resonator. Authors: George N. Saddik, and Robert A. York, MRS Conference April 2011
2. MTT-S IMS Conference June 2011. Title: Capacitively coupled DC voltage switchable barium strontium titanate solidly mounted resonator filter. G. N. Saddik, and R A. York
3. ISAF Conference July 2011. Title: An L-section DC electric field switchable bulk acoustic wave solidly mounted resonator filter based on $Ba_{0.5}Sr_{0.5}TiO_3$. G. N. Saddik, and R A. York
4. G. N. Saddik, and R A. York, "An L-Section DC Electric Field Switchable Bulk Acoustic Wave Solidly Mounted Resonator Filter Based On $Ba_{0.5}Sr_{0.5}TiO_3$," *IEEE Trans. Ultrasonics, Ferroelectrics, and Frequency Control,* vol. 59, No. 9, pp. 2036-2041, Sept 2012
5. George N. Saddik, and Robert A. York, "Temperature Dependence of DC Voltage Activated Switchable $Ba_{0.5}Sr_{0.5}TiO_3$ Solidly Mounted Resonator," *2012 IEEE MTT-S Int. Microwave Symp. Dig.*, June 2012.
6. George N. Saddik and Robert A. York, "Non-Linear Behavior of Voltage Activated BulkAcoustic Wave Resonators Based on $Ba_{0.5}Sr_{0.5}TiO_3$" ISIF 2012 Conference June 2012.
7. George N. Saddik, and Robert A. York, "Impact of Chemical Mechanical Polishing on The Quality Factor of $Ba_{0.5}Sr_{0.5}TiO_3$ Solidly Mounted Resonator," 2013 IEEE MTT-S Int. Microwave Symp. Dig., June 2013..